Journal of Medicinal Chemistry

pubs.acs.org/jmc

Article

Development of an *In Silico* Prediction Model for P-glycoprotein Efflux Potential in Brain Capillary Endothelial Cells toward the Prediction of Brain Penetration

Reiko Watanabe,*,# Tsuyoshi Esaki,# Rikiya Ohashi,* Masataka Kuroda, Hitoshi Kawashima, Hiroshi Komura, Yayoi Natsume-Kitatani, and Kenji Mizuguchi

Cite This: *J. Med. Chem.* 2021, 64, 2725−2738

Read Online

ACCESS | Metrics & More | Article Recommendations | Supporting Information

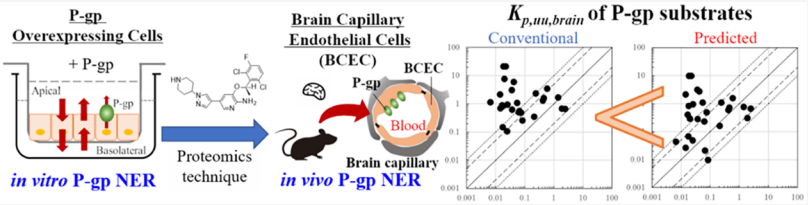

ABSTRACT: Developing *in silico* models to predict the brain penetration of drugs remains a challenge owing to the intricate involvement of multiple transport systems in the blood brain barrier, and the necessity to consider a combination of multiple pharmacokinetic parameters. P-glycoprotein (P-gp) is one of the most important transporters affecting the brain penetration of drugs. Here, we developed an *in silico* prediction model for P-gp efflux potential in brain capillary endothelial cells (BCEC). Using the representative values of P-gp net efflux ratio in BCEC, we proposed a novel prediction system for brain-to-plasma concentration ratio ($K_{p,brain}$) and unbound brain-to-plasma concentration ratio ($K_{p,uu,brain}$) of P-gp substrates. We validated the proposed prediction system using newly acquired experimental brain penetration data of 28 P-gp substrates. Our system improved the predictive accuracy of brain penetration of drugs using only chemical structure information compared with that of previous studies.

■ INTRODUCTION

In the drug discovery of central nervous system (CNS), the design of pharmacologically active drug remains challenging for medicinal chemists.[1] To effectively act in the CNS, a drug must pass through the brain capillary endothelial cells (BCEC) which function as the blood−brain barrier (BBB). In contrast, it is important to limit the brain penetration of non-CNS drugs to avoid unexpected CNS adverse effects. The brain-to-plasma concentration ratio ($K_{p,brain}$) and the unbound brain-to-plasma concentration ratio ($K_{p,uu,brain}$) are generally used as *in vivo* pharmacokinetic (PK) parameters to assess the brain penetration of drugs. As unbound drugs are involved in the exertion of pharmacological and toxicological effects in CNS tissues, it is important to predict the *in vivo* PK parameters for the brain penetration of the drugs by medicinal chemists in the early stages of drug discovery, especially in the drug design process before chemical synthesis, to increase the success rate of drug development.

To predict $K_{p,uu,brain}$ of compounds, it is necessary to consider the involvement of various transporters. P-glycoprotein (P-gp) is a well-characterized efflux transporter at the BBB; it strictly regulates the membrane permeability of substances between the brain tissue and blood by BCEC, pericytes, and astrocytes, as it maintains a low concentration of unbound molecules in the brain relative to that in plasma.[2] In addition, $K_{p,uu,brain}$ is a parameter derived from $K_{p,brain}$. To determine $K_{p,uu,brain}$ from $K_{p,brain}$, PK parameters such as the fraction unbound in brain homogenate ($f_{u,brain}$) and the fraction unbound in plasma ($f_{u,p}$) are required. Previously, we reported individual prediction models for $f_{u,brain}$,[3] $f_{u,p}$,[4] and P-gp net efflux ratio (NER).[5] Furthermore, Rodgers *et al.* proposed a formula to calculate $K_{p,brain}$ using a differential phospholipid method, which mainly considers the physicochemical properties of compounds but does not take into account the involvement of transporters.[6,7] It is necessary to integrate the above-described prediction models to predict brain penetration, which involves a complex mechanism; there are several issues to resolve during the construction of models and the validation of results.

In vivo $K_{p,brain}$ values in mice correlate linearly with the *in vitro* P-gp NER. In addition, Summerfield *et al.* reported a significant improvement in the correlation of $K_{p,brain}$ values between wild-type (WT) and P-gp knock out (KO) mice when

Received: November 20, 2020
Published: February 23, 2021

Downloaded via 65.21.193.86 on February 24, 2022 at 16:53:42 (UTC).
See https://pubs.acs.org/sharingguidelines for options on how to legitimately share published articles.

ACS Publications

© 2021 The Authors. Published by American Chemical Society

https://dx.doi.org/10.1021/acs.jmedchem.0c02011
J. Med. Chem. 2021, 64, 2725−2738

Scheme 1. (A) Overview for Model Building; (B) Validation of the Correction Method for the Prediction of $K_{p,uu,brain}$ from Chemical Structure Information

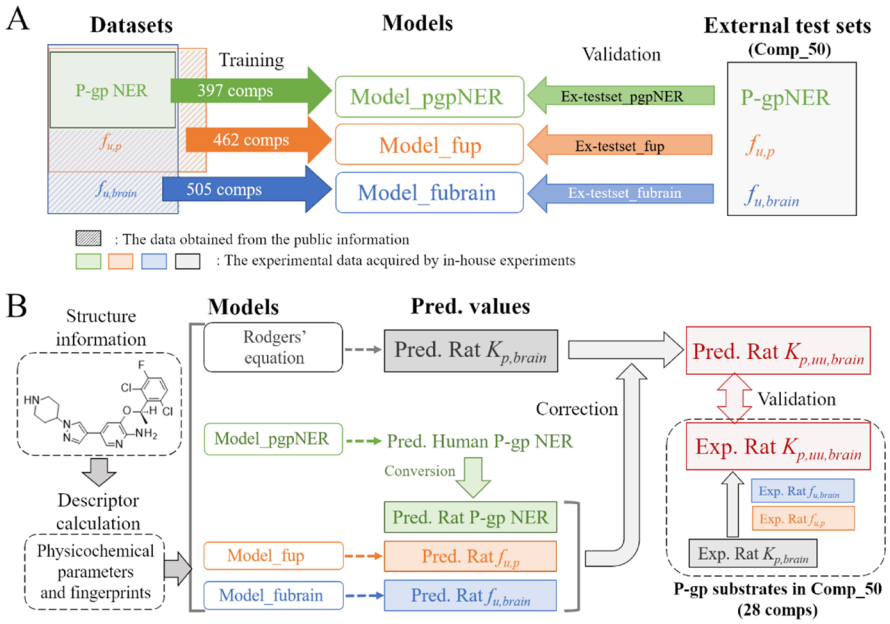

the $K_{p,brain}$ value in the P-gp KO mice was corrected using *in vitro* P-gp NER. However, their calculations indicated that this correction was insufficient to allow extrapolation from WT mice to P-gp KO mice.[8] A possible explanation for the differences between the *in vivo* and *in vitro* results is that P-gp protein expression levels differ between P-gp-overexpressing cell lines and BCEC.[9] A previous study has reported differences in the expression levels of several transporters, not only between species but also between *in vivo* BCEC and *in vitro* cell lines, indicating the difficulty in the direct extrapolation of findings between *in vivo* and *in vitro*.[10]

To overcome these challenges, a strategy to determine transporter protein expression of *in vitro* and *in vivo* experimental compounds using the proteomics technique was proposed and its application in reconstructing *in vivo* P-gp function in both mice and human BCEC was demonstrated.[11−15] Their findings show that the reconstructed P-gp NER is similar to the *in vivo* P-gp NER at the BBB. Their study clarified the functional differences in BBB transport between *in vitro* and *in vivo* models and between human and animal models. However, it has not been verified whether the *in vivo* P-gp function can be reconstructed using the predicted value.

Unlike the predictive models for simple *in vitro* PK parameters such as $f_{u,p}$ and $f_{u,brain}$, $K_{p,brain}$ or $K_{p,uu,brain}$ cannot be routinely verified in humans due to ethical constraints, a limited number of post-mortem determinations, and limited access to imaging analysis systems such as positron emission tomography. Thus, to develop CNS drugs, the $K_{p,brain}$ or $K_{p,uu,brain}$ values obtained using *in vivo* PK experiments in rodents are used as the substitute for experiments in humans, with the expectation that they would show similarities between rodents and humans. However, such expectations ignore potential problems associated with the assumptions that there is no species difference in the transport potential of substrates and that the $K_{p,brain}$ and $K_{p,uu,brain}$ values of rodents are similar to those of humans. Handling species differences remains an important issue.

In the present study, we developed prediction models for P-gp NER as well as for $f_{u,p}$ and $f_{u,brain}$, and obtained the representative values of P-gp NER in human and rat BCEC based on the classification results of a human P-gp NER model. Herein, we propose a novel prediction system for $K_{p,brain}$ and $K_{p,uu,brain}$ using predicted $f_{u,p}$ and $f_{u,brain}$ and the representative value of *in vivo* P-gp NER in rat BCEC instead of the numerical value of P-gp NER in rat BCEC. Using this system, we demonstrated its potential to predict $K_{p,brain}$ and $K_{p,uu,brain}$ solely *via* chemical structure information and showed that the prediction accuracy of $K_{p,uu,brain}$ was superior to that of the conventionally calculated $K_{p,uu,brain}$. The proposed prediction system is open to the public, and this method can have a beneficial effect on CNS drug design before chemical synthesis during the early stages of drug discovery.

■ RESULTS AND DISCUSSION

Study Design Settings and an Overview of Analysis for Model Construction. The study design and an overview of analysis for model construction are presented in Scheme 1. Initially, three prediction models for *in vitro* P-gp NER, $f_{u,p}$, and $f_{u,brain}$ were generated using the datasets obtained from in-house experiments and publicly available data (Model_pgp-NER, Model_fup, and Model_fubrain). Next, we selected 50 diverse compounds from approved drugs that have been reported to be non-P-gp or P-gp substrates, and non-CNS or CNS drugs (Comp_50). The three constructed models were validated using $f_{u,brain}$, $f_{u,p}$ and P-gp NER values (Ex-testset_fubrain, Ex-testset_fup, and Ex-testset_pgpNER), newly obtained from in-house experiments, for the compounds in Comp_50 (Scheme 1A). Finally, we proposed a prediction method for $K_{p,uu,brain}$ considering the efflux transport by P-gp; from the $K_{p,brain}$ predicted using Rodgers' equation, $K_{p,uu,brain}$ was calculated based on predicted P-gp NER, $f_{u,p}$, and $f_{u,brain}$. We experimentally obtained $K_{p,brain}$ and $K_{p,uu,brain}$ for 28 P-gp substrates in Comp_50 and validated the prediction results (Scheme 1B). Therefore, predicting the $K_{p,uu,brain}$ value from the structural information is not accomplished in one-step, but

https://dx.doi.org/10.1021/acs.jmedchem.0c02011
J. Med. Chem. 2021, 64, 2725−2738

Table 1. Basic Dataset Information for P-gp NER, $f_{u,brain}$, and $f_{u,p}$ Predictions

parameter	dataset	species	no. of compounds	range	source
$f_{u,brain}$	Dataset_fubrain	rat	505	0.001−1	in-house data Esaki *et al.*[3]
$f_{u,p}$	Dataset_fup	rat	462	0.001−1	in-house data ChEMBL
P-gp NER	Dataset_pgpNER	human	397	0.29−320	in-house data

Table 2. Statistical Results of Prediction Models in the Condition Examination

parameter	type	validation/test	MSE	r^2	kappa
$f_{u,brain}$	reg.	validation	1.11 ± 0.29	0.65 ± 0.08	
		test	1.48 ± 0.18	0.58 ± 0.06	
$f_{u,p}$	reg.	validation	1.42 ± 0.27	0.58 ± 0.06	
		test	1.70 ± 0.51	0.51 ± 0.11	
P-gp NER	reg.	validation	0.80 ± 0.22	0.34 ± 0.19	
		test	0.95 ± 0.22	0.26 ± 0.14	
	class	validation			0.60 ± 0.12
		test			0.44 ± 0.17

it is a complex process with multiple steps using the four PK parameters.

Generation of Training Datasets for $f_{u,brain}$, $f_{u,p}$, and P-gp NER Prediction. Training datasets for $f_{u,brain}$, $f_{u,p}$, and P-gp NER prediction, containing 505, 462, and 397 compounds, respectively, were constructed from in-house experiments, publicly available data in ChEMBL, and previous study findings, as described in Supporting Information 2. Data were carefully curated to acquire the highest quality possible, as described previously.[4,16] The final number of compounds in datasets, range of parameters, and data sources are shown in Table 1; the datasets for, $f_{u,brain}$, $f_{u,p}$, and P-gp NER prediction were defined as Dataset_pgpNER, Dataset_fubrain, and Dataset_fup, respectively; final data are presented in Supporting Information 1.

Construction of Three Prediction Models. We aimed to construct regression models with Dataset_pgpNER, Dataset_fubrain, and Dataset_fup; details of model construction are shown in Supporting Supporting Information 2, and an overview of the prediction model construction process is shown in Scheme S1 (Supporting Information 3). Initially, the conditions for prediction model construction were examined and then the model was finalized using all the data in the best condition during the initial step. All training steps were performed with 5-fold cross validation. To eliminate the influence of the split bias on the result, 10 patterns of dataset were created by random splitting, and the averages of mean square error (MSE) on the common test sets, along with their standard deviation, were compared as an evaluation metric in the regression among four types of algorithms. The best condition selected following condition examination was set with gradient boosting (GB) as a machine-learning algorithm with feature selection using Boruta, in the logarithmic scale. GB is one of the ensemble-learning methods using multiple weak prediction models. At each stage of parameter optimization, the parameters are updated using the gradient descent method to bring the predictions closer to the observed values. Boruta is an all-relevant feature selection wrapper algorithm designed to automatically perform feature selection on a dataset using random forest. The average of MSE and coefficient of determination (r^2) in the best condition for $f_{u,brain}$ and $f_{u,p}$ in the validation and test sets in the initial step of condition examination are shown in Table 2, and the statistical results of individual models are shown in Table S1 in Supporting Information 3. The finalized models, using all the data in the dataset with the best condition showing the lowest MSE during validation, were selected as the best final prediction model of $f_{u,brain}$, $f_{u,p}$, and P-gp NER. For $f_{u,brain}$ and $f_{u,p}$, the finalized models were defined as Model_fubrain and Model_fup. The regression model for P-gp NER did not show sufficient accuracy as shown in Tables 2 and S1; we also tried to construct a 3-class classification model to distinguish the transport potential of P-gp substrate as a substitute for the regression models based on a previously reported method.[5] The thresholds in Dataset_pgpNER were set to 1.4 and 9.8, as described in the Experimental Section. Splitting the dataset into three classes according to the transport potential of P-gp substrate (low, middle, and high) based on thresholds resulted in 187, 153, and 57 compounds, respectively. Quadratic weighted κ (κ) was used as the evaluation metric (Table 2), and the finalized model was defined as Model_pgpNER.

Validation of the Finalized Prediction Models. The validation data for $f_{u,brain}$, $f_{u,p}$, and P-gp NER were experimentally obtained with 46, 45, and 50 compounds, respectively, from Comp_50 and defined as Ex-testset_fubrain, Ex-testset_fup, and Ex-testset_pgpNER, respectively. The finalized prediction models (Model_fubrain, Model_fup, and Model_PgpNER) were validated using these external datasets. The statistical results of the external test sets are shown in Table 3, and the plots are shown in Figure S1. The prediction accuracy of Ex_testset_fubrain was evaluated using Model_fubrain and our previously reported model (Model_fubrain_prev).[3] Out of the 46 compounds, 10 were excluded during evaluation using Model_fubrain_prev as they were included in the training set of Model_fubrain_prev. The MSE of Model_fubrain was lower than that of Model_fubrain_prev

Table 3. Validation Results of the Prediction Models in the External Dataset of $f_{u,brain}$ and $f_{u,p}$

parameter	data	model	MSE	% within 3-fold error
$f_{u,brain}$	Ex_testset_fubrain	Model_fubrain	1.10	71.7
	Ex_testset_fubrain	previously published model[3]	1.48	46.7
$f_{u,p}$	Ex_testset_fup	Model_fup	1.66	66.7
	Ex_testset_fup	%rat_fup	2.07	57.8

https://dx.doi.org/10.1021/acs.jmedchem.0c02011
J. Med. Chem. 2021, 64, 2725−2738

Table 4. Confusion Matrix of Model_pgpNER[a]

Dataset	κ	exp.	prediction L	prediction M	prediction H	L to H (%)	H to L (%)	L to M (%)	H to M (%)	M to H (%)	M to L (%)
Ex_testset_pgpNER	0.45	L	10	2	1						
		M	7	11	4	7.7	13.3	15.4	46.7	18.2	31.2
		H	2	7	6						

[a]L, low; M, middle; and H, high.

(1.10 *vs* 1.48), and the percentage of samples within 3-fold error increased from 46.7 to 71.7%, indicating that the versatility of our model for $f_{u,brain}$ prediction had improved. Forty-five compounds in Ex_testset_fup were then predicted using Model_fup and %rat_fup model in the ADMET Predictor (Simulations Plus, Lancaster, CA, U.S.A.), which is one of the most widely used commercial software. The MSEs were 1.66 and 2.07, and sample percentages within 3-fold error were 66.7 and 57.8%, for the Model_fup and %rat_fup, respectively. Model_fup presented a slightly better result than %rat_fup, and the prediction accuracy, especially in the lower range of $f_{u,p}$, was higher in Model_fup, as shown in Figure S1B. When the degree of plasma protein binding is high, small differences in protein binding can have large effects on $f_{u,p}$, and thus, the drug efficacy can change dramatically. Therefore, a model with a good prediction accuracy in a low range of $f_{u,p}$ may be more effective during drug development.

The confusion matrix of Model_pgpNER with Ex_testset_pgpNER is shown in Table 4. The κ value for Ex_testset_pgpNER was 0.45. In the three-class classification model, misclassification across two categories should be avoided the most; specifically, a high-potential compound being predicted as a low-potential compound and *vice versa*, these judgment error rates were 7.7 and 13.3%, respectively, with the ex_testset_pgpNER.

Reconstruction from *In Vitro* P-gp NER in P-gp-Overexpressing Cells to P-gp NER in BCEC. We translated the *in vitro* P-gp NER in P-gp-overexpressing cells using in-house experiments data into P-gp NER in BCEC based on the translation method proposed by Uchida *et al.*[9] The details are shown in "Estimation of the P-gp NER in BCEC" of the Experimental Section. The experimentally obtained *in vitro* human and rat P-gp NER values with 48 compounds were used in this analysis. Equation 1 was used to translate *in vitro* human P-gp NER into P-gp NER in human BCEC and eq 2 was used to translate *in vitro* rat P-gp NER into P-gp NER in rat BCEC. The plot illustrating the relationship between *in vivo* P-gp NER in human and rat BCEC is shown in Figure 1. Compounds that showed lower P-gp NER in humans tend to show lower P-gp NER in rats, and compounds that are good substrates in humans had up to 10 times higher NER in rats. In addition, the experimental P-gp NER values in human and rat BCEC were significantly positively correlated (R = 0.72), which is in agreement with the finding of previous studies.[15,17] The regression equation [$y = (x + 0.0119)/0.6533$] was obtained and set as eq 3.

Setting of Representative Values of P-gp NER. To supplement the drawbacks that the numerical value cannot be predicted in the three-class classification model of P-gp NER, we used representative values of P-gp NER in rat BCEC for the prediction of brain penetration. The details are shown in Scheme 2. Initially, the median values of experimental *in vitro* human P-gp NER in the class of P-gp-mediated efflux potential (2.6 and 18.9 in middle and high classes) were converted into

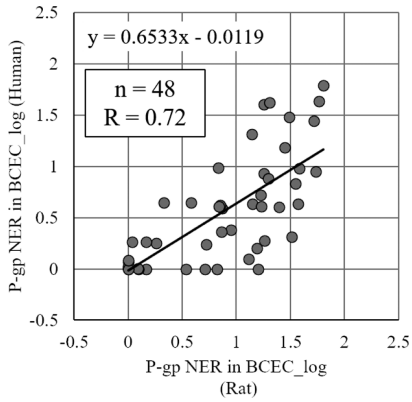

Figure 1. Correlation of the reconstructed P-gp NER between rat and human BCEC. The regression equation (eq 3) is shown in the top left corner; the number of compounds (n) and regression coefficient (R) are also shown. The solid line represents regression.

the representative value of *in vivo* P-gp NER in human BCEC using eq 1 (1.6 and 8.2 in middle and high classes). The representative values of *in vivo* P-gp NER in humans were then converted to those in rats using eq 3. Finally, the representative values of *in vivo* P-gp NER in rat BCEC were set to 2.2 and 26.3 for the middle and high classes, respectively. Furthermore, we used 1.0 as the representative value for the low class, as it is categorized as a P-gp non-substrate.

To the best of our knowledge, we have demonstrated, for the first time, that the representative value of P-gp NER in human and rat BCEC from only compound structure information, can be predicted by unifying the predicted transport potential of the P-gp substrate using Model_pgp-NER. We also proposed a method to translate from *in vitro* P-gp NER in P-gp overexpressing cells to P-gp NER in BCEC. In a previous study, the MDCK-MDR1 cell line from the National Institutes of Health showed higher P-gp expression than that obtained from the Netherlands Cancer Institute.[18] This illustrates the need for validating *in vitro* systems before applying it to CNS drug discovery.[19] Thus, the advantage of predicting the P-gp NER in BCEC is that it can identify *in vivo* P-gp NER directly without considering the differences in the P-gp expression levels among cell lines.

Relationship between $K_{p,uu,brain}$ and Physicochemical/PK Properties. Experimental $K_{p,brain}$ and $K_{p,uu,brain}$ values in WT rats were obtained from experimentally acquired plasma and brain concentration data using eq 4 with 83 compounds, and the relationship between $K_{p,uu,brain}$ and physicochemical properties as well as between PK parameters was analyzed. $f_{u,p}$, $f_{u,brain}$, P-gp NER, and nine physicochemical properties, all of which are generally considered to be important parameters for synthetic expansion, were compared in three parts: $K_{p,uu,brain} < 0.1$, $0.5 \leq K_{p,uu,brain}$, and in-between. The box plots are shown in Figure 2; the molecular weight (MW), topological polar surface area (TopoPSA), number of hydrogen bond acceptors

https://dx.doi.org/10.1021/acs.jmedchem.0c02011
J. Med. Chem. 2021, 64, 2725−2738

Scheme 2. Calculation Process of Representative Values in P-gp NER through the Thresholds of the P-gp NER Prediction Model

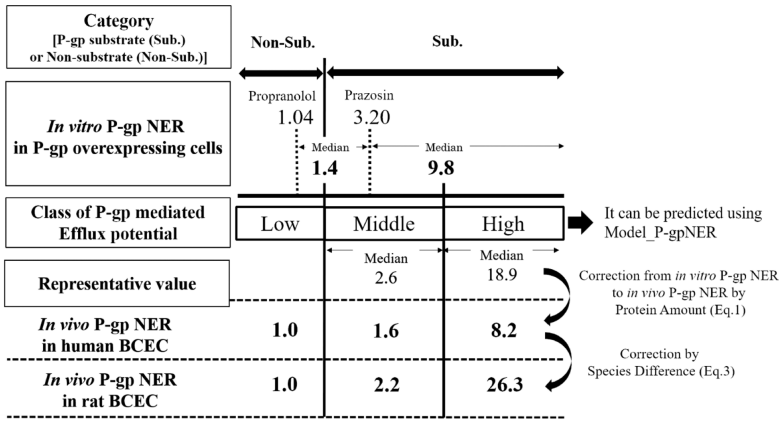

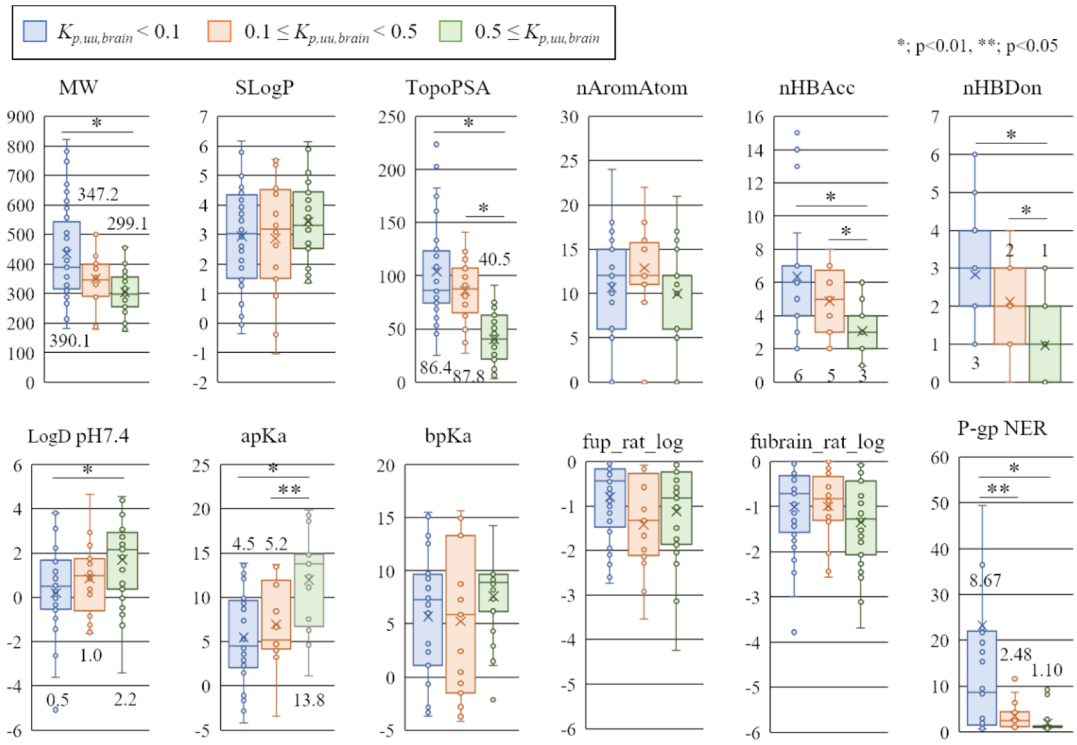

Figure 2. Comparison of 12 physicochemical and PK properties between the degrees of $K_{p,uu,brain}$. The compounds that were 0.1 > $K_{p,uu,brain}$ (n = 36), 0.1 ≤ $K_{p,uu,brain}$ < 0.5 (n = 16), and 0.5 ≤ $K_{p,uu,brain}$ (n = 31) are shown in blue, orange, and green boxes, respectively. *, p < 0.01; **, p < 0.05; cross mark, mean; the numbers above and below the bars indicate the median of the parameters that show significant differences.

(nHBAcc), number of hydrogen bond donors (nHBDon), log D pH 7.4, acidic pK_a (apK_a), and P-gp NER showed significant differences between compounds in $K_{p,uu,brain}$ < 0.1 and 0.5 ≤ $K_{p,uu,brain}$. The median values for the group 0.5 ≤ $K_{p,uu,brain}$ that has a tendency to achieve better brain penetration were MW = 299.1 Da, TopoPSA = 40.5 Å^2, nHBAcc = 3, nHBDDon = 1, log D = 2.2, apK_a = 13.8, and P-gp NER = 1.10.

Correction of $K_{p,brain}$ Value in P-gp KO Rats Using the P-gp NER in Rat BCEC. To effectively validate whether the prediction method for $K_{p,brain}$ and $K_{p,uu,brain}$ that takes into account the influence of P-gp-mediated efflux transport using P-gp NER functions, we obtained experimental $K_{p,brain}$ in P-gp KO rats for 46 compounds, which overlap with the 83 compounds' $K_{p,brain}$ value that were previously acquired in WT rats. $K_{p,brain}$ values of P-gp KO rats were then corrected with three different types of P-gp NERs:[20] (1) numerical P-gp NER in rat BCEC derived from eq 5 (Figure 3B), (2) representative values of rat BCEC according to the classification of experimental P-gp NER using eq 6 (Figure 3C), and (3) representative values of rat BCEC according to the predicted class by Model_pgpNER (Figure 3D).

The $K_{p,brain}$ values in WT and P-gp KO rats are plotted in Figure 3A, with higher $K_{p,brain}$ values observed in P-gp KO rats, demonstrating the influence of P-gp-mediated efflux transport. The samples were classified as either P-gp substrate (P-gp NER ≥ 1.4) or non-substrate (P-gp NER < 1.4) according to the results of our *in vitro* rat P-gp NER study, which showed that 33 and 13 of the compounds were P-gp substrates and non-substrates, respectively. As shown in Figure 3B, the $K_{p,brain}$ value in the P-gp KO rat was corrected using P-gp NER

https://dx.doi.org/10.1021/acs.jmedchem.0c02011
J. Med. Chem. 2021, 64, 2725−2738

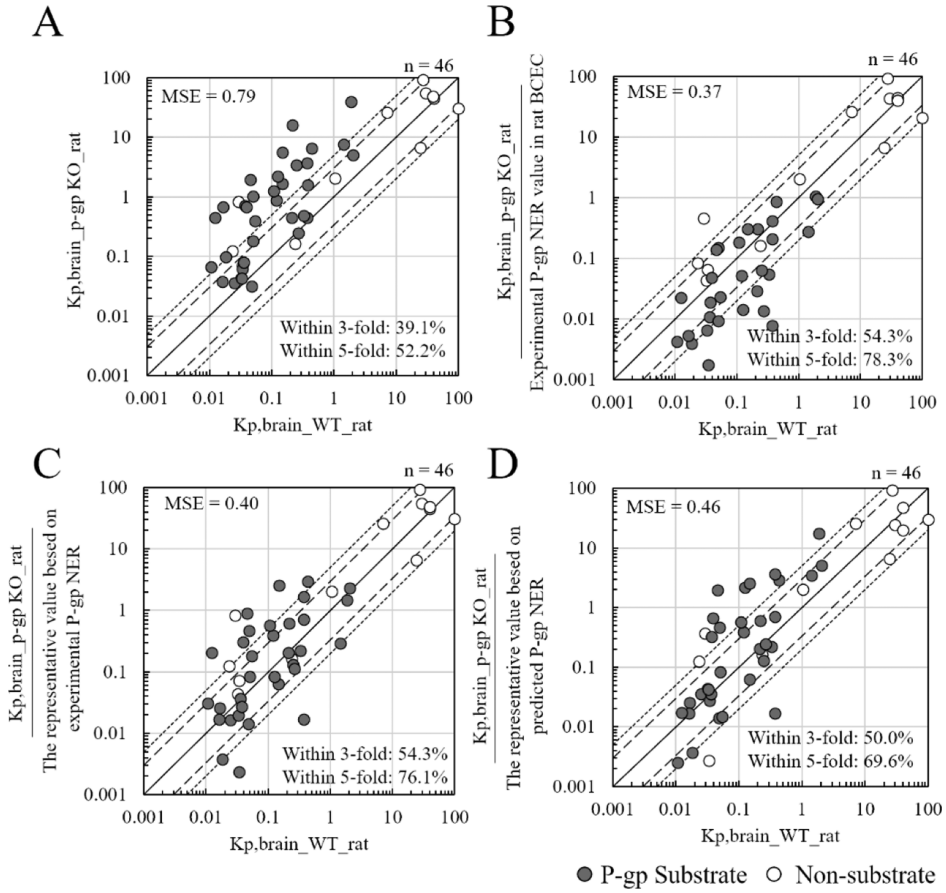

Figure 3. Plot showing the experimental $K_{p,brain}$ values in WT and (A) experimental $K_{p,brain}$ value in P-gp KO rat without correction; (B) corrected $K_{p,brain}$ using the experimental P-gp NER numerical values in rat BCEC reconstructed from *in vitro* rat P-gp NER; (C) corrected $K_{p,brain}$ using the representative value of P-gp NER in rat BCEC based on experimental P-gp NER numerical values; (D) corrected $K_{p,brain}$ using the representative value of P-gp NER in rat BCEC based on the predicted class with Model_pgpNER. P-gp substrates and non-substrates are indicated in gray and white circles, respectively. The MSE is shown in top left corners. The percentage of samples with a 3- or 5-fold error is shown at the bottom. Straight, dashed, and dotted lines indicate the lines of unity, 3-fold and 5-fold errors, respectively (n = 46).

numerical values in rat BCEC with eq 5. The MSE decreased from 0.79 to 0.37, and the percentage of P-gp substrates that fell within a 5-fold error increased from 52.2 to 78.3%. These results indicate that the P-gp NER in rat BCEC reconstructed using *in vitro* P-gp NER could be used quantitatively to account for the brain penetration observed *in vivo* relative to that in P-gp KO models, as reported previously.[9]

As shown in Figure 3C, the $K_{p,brain}$ correlated with the representative values of rat BCEC according to the classification of experimental P-gp NER using eq 6. The percentage of compounds that fell within a 5-fold error increased from 52.2 to 76.1%, accompanied by a decrease in the MSE from 0.79 to 0.40 in all compounds. The effectiveness of correction was equivalent to that observed using experimental values (0.37 *vs* 0.40 in MSE and 78.3 *vs* 76.1% in compounds that fell within a 5-fold error, in the experimental values and the representative values, respectively). These results indicate that the $K_{p,brain}$ value was well corrected by the representative value of P-gp NER.

We then corrected the $K_{p,brain}$ value in P-gp KO rats using the representative values of rat BCEC according to the predicted class using Model_pgpNER (Figure 3D). The percentage of compound that fell within a 5-fold error was 69.6%, the MSE decreased to 0.46, and the effectiveness of correction was slightly lower than that achieved when the experimental values were used. However, approximately 70% of samples fall within a 5-fold error. These results indicate that the $K_{p,brain}$ value could be corrected using the representative values based on the predicted classification of P-gp NER using Model_pgpNER.

Calculation of $K_{p,uu,brain}$ Value Using $K_{p,brain}$, $f_{u,p}$, and $f_{u,brain}$. We calculated $K_{p,uu,brain}$ from the corrected $K_{p,brain}$ in P-gp KO rats, as shown in Figure 3C,D, using the experimental or predicted values of $f_{u,p}$ and $f_{u,brain}$ of 42 compounds using eq 7. The predicted $f_{u,p}$ and $f_{u,brain}$ values were derived from the prediction results of Model_fup with Ex_testset_fup and Model_fubrain with Ex_testset_fubrain. The prediction of $K_{p,uu,brain}$ was evaluated within a 5- or 10-fold variation, as 5-fold experimental variation has been previously reported in the dataset of $K_{p,uu,brain}$ resulting from combining three end points to derive $K_{p,uu,brain}$; $K_{p,brain}$, $f_{u,p}$, and $f_{u,brain}$.[21] Thus, we cannot definitively conclude that there is a significant difference with a 5-fold variation.[22] Obtaining experimental data for $f_{u,p}$, $f_{u,brain}$, and P-gp NER for compounds that are highly adsorbed onto plasma proteins or lipid membrane is technically difficult and might cause a huge experimental error. As these experimental errors affect $K_{p,uu,brain}$ prediction, we considered the standard range to be 5-fold and set 10-fold as the acceptable error range for the evaluation of $K_{p,uu,brain}$ prediction.

https://dx.doi.org/10.1021/acs.jmedchem.0c02011
J. Med. Chem. 2021, 64, 2725−2738

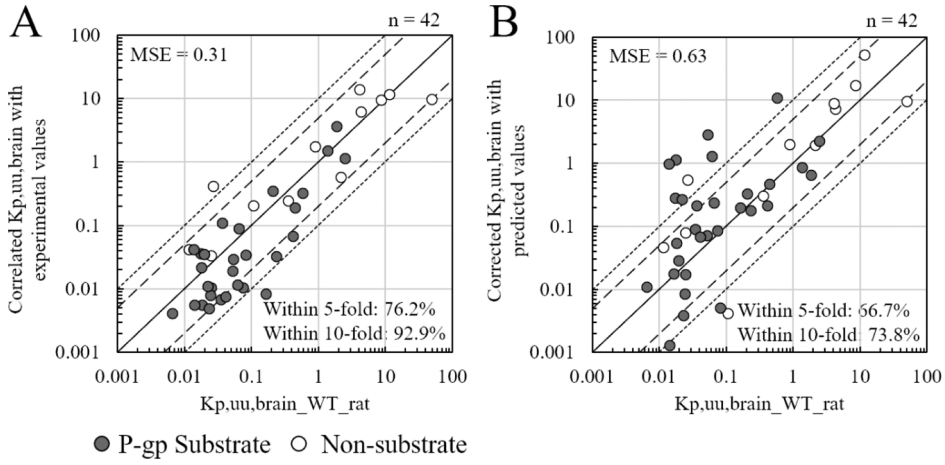

Figure 4. (A) Plot of $K_{p,uu,brain}$ in WT rats and p-gp KO rats calculated using experimental $f_{u,p}$ and $f_{u,brain}$ values. (B) Plot of $K_{p,uu,brain}$ in WT rats and p-gp KO rats calculated using predicted $f_{u,p}$ and $f_{u,brain}$ values. In plots (A,B), P-gp substrates and non-substrates are shown in gray and white circles, respectively. The MSE and number of compounds (n) are shown in the top left and top right corners, respectively. Straight, dashed, and dotted lines indicate the line of unity, 5-fold, and 10-fold errors, respectively.

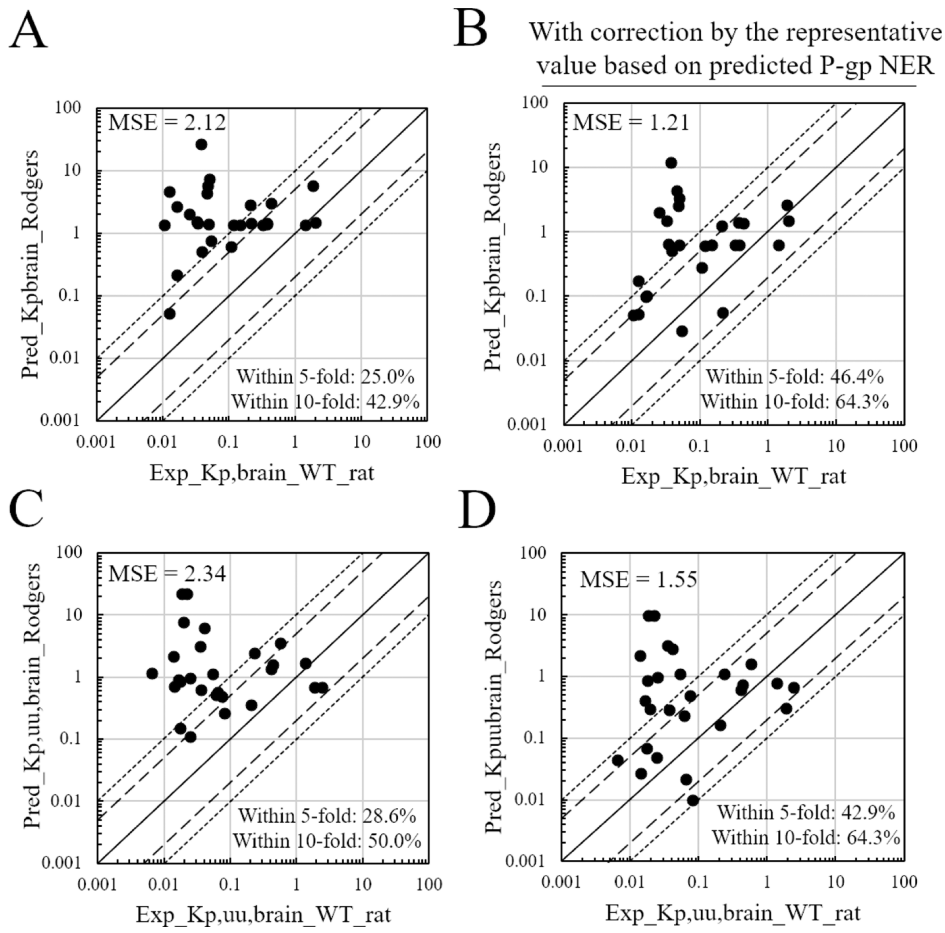

Figure 5. Plot of $K_{p,brain}$ and $K_{p,uu,brain}$ in the P-gp substrate before and after correlation. Experimental $K_{p,brain}$ in WT rats *vs* $K_{p,brain}$ calculated using Rodgers' formula (A), *vs* $K_{p,brain}$ corrected using the representative value based on the predicted P-gp NER (B). Experimental $K_{p,uu,brain}$ in WT rats *vs* $K_{p,uu,brain}$ calculated from $K_{p,brain}$ without correction (C) and *vs* corrected $K_{p,uu,brain}$ (D) with the predicted $f_{u,p}$ and $f_{u,brain}$ values. P-gp substrates (n = 28) are plotted. Straight, long-dashed, and dotted lines indicate the line of unity, 5-fold and 10-fold errors, respectively.

Figure 4 shows the plots of $K_{p,uu,brain}$ value corrected using the representative values based on experimental and predicted P-gp NER in rat BCEC, and experimental and predicted $f_{u,p}$ and $f_{u,brain}$ data. With the experimental value, MSE and the percentage of compounds that fell within 5-fold and 10-fold errors were 0.31, 76.2, and 92.9%, respectively, indicating that $K_{p,uu,brain}$ can be predicted using the correction of $K_{p,brain}$ by P-gp NER in rat BCEC. The predicted data revealed that the MSE and the percentage of compounds fell within 5- and 10-fold errors were 0.63, 66.7, and 73.8%, respectively. We

https://dx.doi.org/10.1021/acs.jmedchem.0c02011
J. Med. Chem. 2021, 64, 2725−2738

Table 5. Difference between the Experimental and Predicted Values of P-gp NER, $f_{u,p}$, $f_{u,brain}$, $K_{p,brain}$, and $K_{p,uu,brain}$ in 28 P-gp Substrates for Validation

Compound structure	Compound name	P-gp NER		$f_{u,p}$		$f_{u,brain}$		$K_{p,brain}$		$K_{p,uu,brain}$	
		Exp. (Value)	Pred.	Exp.	Pred. (Fold error)	Exp.	Pred. (Fold error)	Exp. $K_{p,brain}$ in KO rat	Calculated $K_{p,brain}$ (Fold error)	Exp.	Pred. (Fold error)
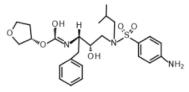	Amprenavir[a]	Middle (8.781)	High	0.129	0.101 (1.3)	0.204	0.169 (1.2)	0.452	4.587 (10.2)	0.020	0.292 (14.9)
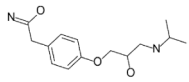	Atenolol[a]	Middle (1.987)	Low	1.000	1.396 (1.4)	1.000	0.664 (1.5)	0.036	2.033 (56.5)	0.025	0.967 (38.8)
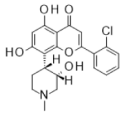	Alvocidib	Middle (6.848)	Middle	0.051	0.044 (1.2)	0.057	0.038 (1.5)	0.451	2.778 (6.2)	0.234	1.093 (4.7)
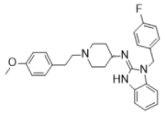	Astemizole	High (15.621)	Middle	0.011	0.019 (1.7)	0.004	0.012 (3.3)	38.935	5.694 (6.8)	0.577	1.585 (2.7)
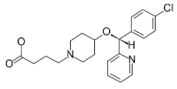	Bepotastine[a]	Middle (1.459)	Middle	0.642	0.019 (34.3)	0.245	0.072 (3.4)	0.031	5.628 (180.5)	0.018	9.857 (539)
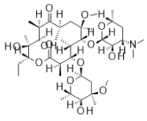	Clarithromycin[a]	Middle (6.230)	Low	0.377	0.472 (1.3)	0.113	0.236 (2.1)	1.955	4.356 (2.2)	0.014	2.175 (157.7)
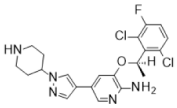	Crizotinib	Middle (7.903)	Middle	0.030	0.047 (1.6)	0.003	0.005 (1.5)	5.546	1.363 (4.1)	0.017	0.069 (4.0)
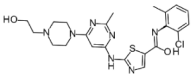	Dasatinib[a]	High (14.882)	Middle	0.026	0.044 (1.7)	0.013	0.028 (2.2)	0.061	1.414 (23.2)	0.016	0.412 (25.1)
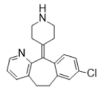	Desloratadine	High (11.901)	Middle	0.190	0.017 (10.9)	0.008	0.006 (1.2)	7.607	1.364 (5.6)	0.061	0.232 (3.8)
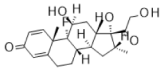	Dexamethasone	Middle (7.449)	High	0.159	0.269 (1.7)	0.238	0.093 (2.6)	0.391	0.752 (1.9)	0.081	0.01 (8.2)
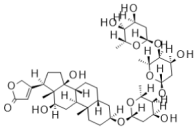	Digoxin[a]	Middle (6.287)	Low	0.583	0.119 (4.9)	0.264	0.201 (1.3)	0.674	0.503 (1.3)	0.018	0.849 (48.0)
	Disopyramide	Middle (3.368)	Middle	0.669	0.123 (5.4)	0.491	0.056 (8.7)	1.022	1.390 (1.4)	0.036	0.287 (7.9)
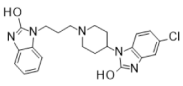	Domperidone[a]	High (16.056)	Middle	0.029	0.056 (1.9)	0.017	0.046 (2.6)	0.714	26.395 (37.0)	0.022	9.893 (448.2)

https://dx.doi.org/10.1021/acs.jmedchem.0c02011
J. Med. Chem. 2021, 64, 2725−2738

Table 5. continued

Compound structure	Compound name	P-gp NER		$f_{u,p}$		$f_{u,brain}$		$K_{p,brain}$		$K_{p,uu,brain}$	
		Exp. (Value)	Pred.	Exp.	Pred. (Fold error)	Exp.	Pred. (Fold error)	Exp. $K_{p,brain}$ in KO rat	Calculated $K_{p,brain}$ (Fold error)	Exp.	Pred. (Fold error)
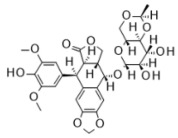	Etoposide	Middle (3.455)	Middle	0.357	0.129 (2.8)	0.539	0.065 (8.3)	0.037	0.215 (5.8)	0.024	0.049 (2.0)
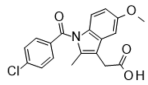	Indometacin	Middle (2.673)	Low	0.008	0.010 (1.2)	0.048	0.093 (1.9)	0.009	0.052 (5.7)	0.074	0.489 (6.6)
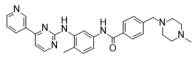	Imatinib*	Middle (8.543)	Middle	0.045	0.026 (1.7)	0.037	0.022 (1.7)	0.182	7.400 (40.6)	0.041	2.789 (68.1)
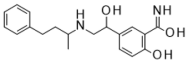	Labetalol*	Middle (7.840)	Low	0.519	0.168 (3.1)	0.075	0.131 (1.8)	3.677	1.415 (2.6)	0.054	1.107 (20.7)
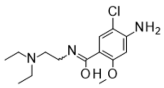	Metoclopramide	Middle (2.731)	Low	0.677	0.332 (2.0)	0.817	0.150 (5.5)	5.050	1.493 (3.4)	2.454	0.674 (3.6)
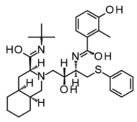	Nelfinavir	High (26.267)	High	0.003	0.034 (13.5)	0.001	0.015 (14.8)	0.668	2.662 (4.0)	0.007	0.044 (6.8)
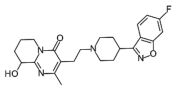	Paliperidone	Middle (7.435)	Middle	0.047	0.046 (1.0)	0.176	0.054 (3.3)	0.867	1.354 (1.6)	0.443	0.726 (1.6)
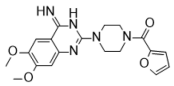	Prazosin	Middle (7.946)	Low	0.264	0.135 (2.0)	0.163	0.109 (1.5)	0.247	1.364 (5.5)	0.164	1.1 (6.7)
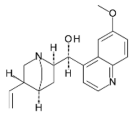	Quinidine	High (21.799)	High	0.243	0.169 (1.4)	0.073	0.066 (1.1)	15.895	1.455 (10.9)	0.065	0.021 (3.0)
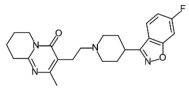	Risperidone	Middle (2.133)	Middle	0.033	0.044 (1.3)	0.120	0.054 (2.2)	1.565	1.377 (1.1)	1.378	0.768 (1.8)
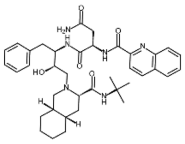	Saquinavir	Middle (7.041)	High	0.005	0.051 (10.4)	0.006	0.026 (4.0)	0.067	1.351 (20.2)	0.014	0.026 (1.9)
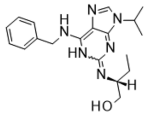	Seliciclib	Middle (3.399)	Middle	0.048	0.203 (4.2)	0.092	0.117 (1.3)	1.259	0.616 (2.1)	0.205	0.162 (1.3)
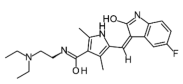	Sunitinib	Middle (4.183)	Middle	0.007	0.070 (9.6)	0.009	0.068 (7.4)	0.481	1.366 (2.8)	0.414	0.605 (1.5)
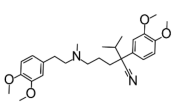	Verapamil	Middle (3.602)	Middle	0.011	0.080 (7.0)	0.049	0.018 (2.7)	6.432	3.020 (2.1)	1.860	0.308 (6.0)

https://dx.doi.org/10.1021/acs.jmedchem.0c02011
J. Med. Chem. 2021, 64, 2725−2738

Table 5. continued

Compound structure	Compound name	P-gp NER		$f_{u,p}$		$f_{u,brain}$		$K_{p,brain}$		$K_{p,uu,brain}$	
		Exp. (Value)	Pred.	Exp.	Pred. (Fold error)	Exp.	Pred. (Fold error)	Exp. $K_{p,brain}$ in KO rat	Calculated $K_{p,brain}$ (Fold error)	Exp.	Pred. (Fold error)
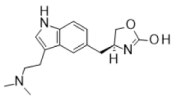	Zolmitriptan[a]	Middle (3.264)	Low	0.942	0.354 (2.7)	1.000	0.741 (1.4)	0.043	1.506 (35.3)	0.035	3.153 (90.6)

[a]10 P-gp substrates whose fold error in $K_{p,uu,brain}$ was more than 10-fold; exp., experimental; pred., predicted; calc., calculated; and fold error, the fold error between the experimental and the predicted/calculated values.

concluded that rat $K_{p,uu,brain}$ could be calculated using our proposed method using representative P-gp NER values in rat BECE. Moreover, the experimental values of P-gp NER, $f_{u,brain}$, and $f_{u,p}$ can be replaced by the predicted results of Model_pgpNER, Model_fubrain, and Model_fup, respectively.

Validation of the Correction Method for the Prediction of $K_{p,uu,brain}$ Using the Calculated $K_{p,brain}$ Value with Rodgers' Equation. For the practical application of the proposed correction method using P-gp NER in BCEC, it is necessary to predict $K_{p,brain}$ according to simple measurements or using only structural information. The result revealed that $K_{p,brain}$ in P-gp KO rats cannot be practically used. Therefore, $K_{p,brain}$ was calculated using a differential phospholipid method proposed by Rodgers *et al.*,[6,7] and the proposed correction method that we evaluated in P-gp KO rats was applied to $K_{p,brain}$ calculated using Rodgers' equation. As the prediction values of $f_{u,p}$ were required for $K_{p,brain}$ calculation with Rodgers' equation, the difference between the experimental values and the calculated $K_{p,brain}$ using the predicted values was analyzed before validating the correction method (Figure S2). We concluded that the observed value can be replaced with predicted values.

Finally, our proposed correction method, using the representative value of P-gp NER in BCEC based on the predicted class with Model_pgpNER, Model_fubrain, and Model_fup, was applied to $K_{p,brain}$ calculated using Rodgers' equation. The results were validated using experimentally acquired $K_{p,brain}$ and $K_{p,uu,brain}$ values of 28 P-gp substrates in Comp_50, as shown in Scheme 1. The MSE decreased from 2.12 to 1.21 for $K_{p,brain}$, and from 2.34 to 1.55 for $K_{p,uu,brain}$ following correction using the predicted P-gp NER in BCEC. The percentage of samples within a 10-fold error increased from 42.9 to 64.3% for $K_{p,brain}$, and from 50.0 to 64.3 for $K_{p,uu,brain}$ (Figure 5A,B). These results indicate that the $K_{p,brain}$ and $K_{p,uu,brain}$ values were predicted only from structural information with better accuracy than the conventional method. Ten compounds, namely, atenolol, amprenavir, bepotastine, clarithromycin, dasatinib, digoxin, domperidone, imatinib, labetalol, and zolmitriptan, had shown substantial error of more than 10-fold (Table 5), and this could be attributed to the accumulation of gaps in the predicted values. The difference between the $K_{p,brain}$ value using Rodgers' equation and the experimental $K_{p,brain}$ in P-gp KO rats appeared to be one of the most influenced factors, because compounds with a larger fold error in calculated $K_{p,brain}$ presented a larger difference in $K_{p,uu,brain}$ prediction. The $K_{p,brain}$ value of atenolol, bepotastine, dasatinib, domperidone, imatinib, saquinavir, and zolmitriptan differed by 14.9−539 times (Table 5). Atenolol, apixaban, dasatinib, imatinib, and zolmitriptan are known as substrates of not only P-gp but also other transporters such as breast cancer resistance protein (BCRP) and organic anion-transporting polypeptide (OATP).[23−27] Although Rodgers' equation is currently the best method to predict tissue-to-plasma partition coefficient, it does not consider the transporters' involvement and prediction accuracy in tissues with a larger contribution of transporters, such as the brain, kidney, and liver, insufficient, especially when the compounds were substrates for multiple transporters. The results also illustrate the difficulty in predicting compounds such as digoxin. Digoxin binds slowly and specifically to its target molecule Na^+/K^+ ATPase, which is ubiquitously expressed in the body. Therefore, digoxin is extensively distributed in tissues and equilibrates slowly.[28,29] In addition, the prediction error in P-gp NER classification also influenced the accuracy of $K_{p,uu,brain}$ prediction. 8 out of 10 compounds were misclassified in Model_pgpNER, suggesting that further improvement in the prediction accuracy of Model_pgpNER is required.

Using the predicted representative value of P-gp NER in BCEC and the predicted $f_{u,brain}$ and $f_{u,p}$ values, we have demonstrated the prediction system for $K_{p,brain}$ and $K_{p,uu,brain}$ from chemical information alone. Although the method proposed in this study is not applicable to all compounds, given that several transporters are involved in brain penetration of drugs, we showed that at least for P-gp substrates, its predictive accuracy for $K_{p,brain}$ and $K_{p,uu,brain}$ by correction using predicted representative P-gp NER increased compared with that for prediction of $K_{p,brain}$ using Rodgers' equation. Other studies have also reported species-specific differences in substrate recognition and transportability, as well as differences in absolute protein expression levels of BCRP and OATP in human and animal brain capillaries.[11−15] This method can be applied to other transporters such as BCRP and OATP when predicting $K_{p,brain}$ and $K_{p,uu,brain}$ for their substrates, making it possible to construct a prediction model that is intended for more compounds.

Possibility of Practical Application for the Prediction of Brain Penetration of Drugs in Humans. As $K_{p,brain}$ and $K_{p,uu,brain}$ values in rodents can be acquired with comparative ease from the drug concentrations in the brain and plasma, $f_{u,p}$ and $f_{u,brain}$, previous studies have reported several predictive models for $K_{p,brain}$ and $K_{p,uu,brain}$ values in rodents using machine-learning techniques.[30−32] However, it is not the best option to directly apply the prediction results in animals to humans; predictive models targeting transporter substrates must consider species-specific differences in transporter protein expression levels and their functions at the BBB.

The rat $K_{p,uu,brain}$ value predicted using machine learning is not directly applicable to humans, whereas the human $K_{p,uu,brain}$

https://dx.doi.org/10.1021/acs.jmedchem.0c02011
J. Med. Chem. 2021, 64, 2725−2738

value can be predicted using our proposed method by replacing the parameters used in rats with those used in humans. We believe that our proposed method can be expanded to include humans; however, the lack of human validation data remains an obstacle. Drug concentration in the cerebrospinal fluid (CSF) is used as a surrogate for cerebral interstitial fluid, as CSF is the only accessible sample in human CNS tissues. Friden *et al.*[30] compared human and rat unbound CSF with the plasma concentration ratio for 32 structurally diverse compounds and demonstrated an association with the brain exposure of species. However, as it is difficult to collect the human CSF data under unified conditions such as health status, time points of CSF sampling, and different CSF sources, it is difficult to distinguish whether the observed difference reflects a true species difference or observational bias. Moreover, several-fold differences between the concentration in the cerebral interstitial fluid and CSF have been reported.[33,34] The lack of reliable concentration data for human cerebral interstitial fluid, which can be used to verify the predicted results, is a major obstacle for future verification of the *in silico* prediction results.

■ CONCLUSIONS

In this study, we initially constructed the regression models of $f_{u,p}$ and $f_{u,brain}$, and the 3-class classification model to distinguish the transport potential of the P-gp substrate accurately based on structural information; then, the representative values of P-gp NER in human and rat BCEC were set. Second, we proposed a new prediction system *via* correction using the representative values of P-gp NER to predict $K_{p,brain}$ and $K_{p,uu,brain}$ in P-gp KO rats, and the system was successfully validated. Finally, we demonstrated that our prediction system can be applied to the calculated $K_{p,brain}$, and after applying our prediction method, the predictive accuracy of $K_{p,brain}$ and $K_{p,uu,brain}$ in P-gp substrates in rats increased. A new web resource (http://adme.nibiohn.go.jp/brain-penetration) has been established to access the online system for the prediction of brain penetration, as described in this study. We believe that our proposed method can be potentially used in CNS drug discovery to estimate the pharmacological effects and optimize the drug candidates at an early stage.

■ EXPERIMENTAL SECTION

Materials. Test compounds were of analytical grade (purity >95%) and purchased from Tokyo Chemical Industry (Tokyo, Japan), MedChemExpress (Monmouth Junction, NJ, U.S.A.), AdooQ Bioscience (Irvine, CA, U.S.A.), Sigma-Aldrich (St. Louis, MO, U.S.A.), ChemScene (Monmouth Junction, NJ, U.S.A.), Fujifilm Wako Pure Chemical Corporation (Osaka, Japan), and Toronto Research Chemicals (North York, Canada). A total of 447 compounds were dissolved at a concentration of 10 mM in 100% DMSO and 1 mg/mL (0.5%, w/v) methyl cellulose for *in vitro* and *in vivo* experiments, respectively. The solutions were stored at 4 °C and used within 2 weeks following preparation.

Acquisition of Experimental Data. P-gp efflux transport in rat and human P-gp-overexpressing cells was measured to evaluate the P-gp substrate potential. LLC-PK1 and LLC-GA5-CoL150 cells were purchased from RIKEN BioResource Research Center (Cell IDs: RCB0558 and RCB0871; Tsukuba, Japan). LLC-GA5-CoL150 cells had been stably transfected with the human MDR1 gene to overexpress P-gp.[35,36] Rat Mdr1a-overexpressing LLC-PK1 cells were prepared by Sekisui Medical Co. Ltd. (Tokyo, Japan). The P-gp expression level in LLC-PK1, LLC-GA5-CoL150, and rat Mdr1a-overexpressing LLC-PK1 cells was determined by Sekisui Medical Co. Ltd. (Tokyo, Japan) as previously described.[7] Plasma and brain homogenate binding were determined using equilibrium dialysis by Sekisui Medical Co. Ltd. (Tokyo, Japan). The measurement of drug concentration in the brain and plasma in WT and P-pg KO rats was performed in Shin Nippon Biomedical Laboratories (SNBL; Tokyo, Japan), and studies were performed in accordance with all institutional guidelines, and the animal study protocol was approved by the Animal Care and Use Committee SNBL (approval numbers: IACUC819-010, IACUC819-011, IACUC819-015, and IACUC819-016). The details of experimental procedures in each experiment are shown in Supporting Information 4.

Threshold of Classification Model for P-gp NER. Thresholds of P-gp NER were established, and the process is shown in Scheme 2. Based on the method proposed by Ohashi *et al.*,[5] propranolol (a non-P-gp substrate; geometric mean NER = 1.04) and prazosin (a weak P-gp substrate; geometric mean NER = 3.20) were included in each experiment as a control compound. The first threshold was determined as the border between the P-gp non-substrate and the P-gp weak substrate using the median of the data between 1.04 and 3.20, which was 1.4. The second threshold was 9.8, determined using the median of compounds to be >3.20 (geometric mean NER of weak substrate). The compounds with P-gp NER less than 1.4 (P-gp NER < 1.4), between 1.4 and 9.8 (1.4 ≤ P-gp NER ≤ 9.8), and more than 9.8 (9.8 < P-gp NER) were defined as low-, middle-, and high-class compounds, respectively.

Estimation of the P-gp NER in BCEC. Previous studies have reported the methodology to reconstruct *in vivo* P-gp function in the BBB (BCEC) from *in vitro* P-gp function in P-gp-expressing cells.[9,10] They demonstrated that the *in vivo* P-gp transport activity (NER) could be extrapolated from *in vitro* P-gp transport activity in P-gp-expressing cells by correction of the P-gp protein expression amount. We measured the P-gp protein expression amount of several cell lines and estimated the *in vivo* P-gp NER in rats from *in vitro* P-gp NER according to these reports. The measured *in vitro* P-gp protein expression amount in rat and human P-gp-overexpressing cells according to a previous protocol[37] were 15.0 and 7.72 fmol/μg protein in human and rat P-gp-overexpressing cells, respectively. Human and rat P-gp protein expressions in BCEC have previously been reported to be 6.06[12] and 19.1[15] fmol/μg protein, respectively. Accordingly, we calculated the human and rat P-gp NER in BCEC using eqs 1 and 2, respectively

$$\text{P-gp NER in human BCEC} = 1 + (\textit{in vitro}\ \text{human P-gp NER} - 1)*\frac{6.06}{15.0} \quad (1)$$

$$\text{P-gp NER in rat BCEC} = 1 + (\textit{in vitro}\ \text{rat P-gp ER} - 1)*\frac{19.1}{7.72} \quad (2)$$

We translated the P-gp NER in human BCEC from *in vitro* human P-gp NER according to eq 1 and then estimated P-gp NER in rat BCEC from P-gp NER in human BCEC according to the correlation, eq 3, in Figure 1

$$\log(\text{P-gp NER in rat BCEC}) = \{(\log(\text{P-gp NER in human BCEC})) + 0.019\}/0.6533 \quad (3)$$

The median of *in vitro* human P-gp NER in middle- and high-class compounds (2.6 and 18.9 in the middle and migh classes, respectively), which were set in "Threshold of Classification Model for P-gp NER" section, were converted to the representative values of P-gp NER in rat BCEC according to eq 3 following the conversion to human P-gp NER in BCEC according to eq 1. The representative value of P-gp NER rat in BCEC for the compounds classified into middle and high classes by the classification model was set to 2.2 and 26.3 in middle and high classes, respectively. Furthermore, we used 1.0 as the final representative value for the compounds classified as low class using the classification model as it does not influence P-gp in low-class compounds.

https://dx.doi.org/10.1021/acs.jmedchem.0c02011
J. Med. Chem. 2021, 64, 2725−2738

Correction of $K_{p,brain}$ and Calculation of $K_{p,uu,brain}$. $K_{p,brain}$ values were calculated using eq 4

$$K_{p,brain} = \frac{C_{brain}}{C_{plasma}} \quad (4)$$

where C_{brain} and C_{plasma} are concentrations of a compound in the brain and plasma, respectively.

The $K_{p,brain}$ value in P-gp KO rats can be corrected to that of WT rat using the following equation described by Summerfield *et al.*[8]

$$\text{corrected } K_{p,brain} = \frac{K_{p,brain}}{\text{the numerical value of P-gp NER in BCEC}} \quad (5)$$

Using eq 5, $K_{p,brain}$ that takes into account the influence of P-gp can be estimated. However, the numerical value cannot be substituted in P-gp NER in BCEC in the prediction process as the quantitative prediction method of P-gp NER could not be constructed. Therefore, in this report, we propose the substitution to the representative values of P-gp NER based on the classification model for P-gp NER instead of the numerical value of P-gp NER in rat BCEC when the corrected $K_{p,brain}$ is calculated using eq 5.

Thus, the $K_{p,brain}$ value was corrected using each representative value calculated using eq 6 in Figure 4

$$\text{corrected } K_{p,brain} = \frac{K_{p,brain}}{\text{the representative value of P-gp NER in BCEC}} \quad (6)$$

The representative values (low = 1, middle = 2.2, or high = 26.3) were set.

Finally, the $K_{p,uu,brain}$ value was calculated as follows

$$K_{p,uu,brain} = \text{corrected } K_{p,brain} \times \frac{f_{u,brain}}{f_{u,plasma}} \quad (7)$$

$K_{p,brain}$ Value Calculated Using Rodgers' Equation. $K_{p,brain}$ was calculated for 28 compounds that are P-gp substrates in the external test set using a differential phospholipid method proposed by Rodgers *et al.*[6,7] The values of four physicochemical/PK parameters, namely, log *P*, pK_a, $f_{u,p}$, and blood to plasma concentration ratio (Rb) were required for the $K_{p,brain}$ calculation using Rodgers' equation. Log *P* and pK_a were acquired from ChEMBL27. As predicted parameters, the Rb value was set to 1.0 and the predicted $f_{u,p}$ value with Model_fup was used. To compare the predicted accuracy of $K_{p,brain}$ when using the predicted values, the experimental $f_{u,p}$ value and the Rb value in rats were obtained.

■ ASSOCIATED CONTENT

Supporting Information

The Supporting Information is available free of charge at https://pubs.acs.org/doi/10.1021/acs.jmedchem.0c02011.

Experimental data and datasets; model construction; process of prediction model construction in $f_{u,brain}$, $f_{u,p}$, and P-gp NER; individual statistical results during condition examination in the construction of prediction models for $f_{u,brain}$, $f_{u,p}$, and P-gp NER; plots of prediction results in Model_fubrain and Model_fup; difference between the experimental values and the calculated $K_{p,brain}$, corrected $K_{p,brain}$, or $K_{p,uu,brain}$ values using predicted values; plot of $K_{p,uu,brain}$ in WT rats versus calculated $K_{p,uu,brain}$ using predicted results; and experimental data acquisition (PDF)

Dataset_pgpNER, Dataset_$f_{u,brain}$, Dataset_$f_{u,p}$, Ex-testset_pgpNER, Ex-testset_$f_{u,brain}$, and Ex-testset_$f_{u,p}$ (XLSX)

■ AUTHOR INFORMATION

Corresponding Authors

Reiko Watanabe − *Laboratory of Bioinformatics, Artificial Intelligence Center for Health and Biomedical Research, National Institutes of Biomedical Innovation, Health and Nutrition, Osaka 567-0085, Japan;* orcid.org/0000-0001-9359-8731; Email: reiko-watanabe@nibiohn.go.jp

Rikiya Ohashi − *Laboratory of Bioinformatics, Artificial Intelligence Center for Health and Biomedical Research, National Institutes of Biomedical Innovation, Health and Nutrition, Osaka 567-0085, Japan; Discovery Technology Laboratories, Mitsubishi Tanabe Pharma Corporation, Fujisawa, Kanagawa 251-8555, Japan*; Email: rikiya-ohashi@nibiohn.go.jp

Authors

Tsuyoshi Esaki − *The Center for Data Science Education and Research, Shiga University, Hikone, Shiga 522-8522, Japan*

Masataka Kuroda − *Laboratory of Bioinformatics, Artificial Intelligence Center for Health and Biomedical Research, National Institutes of Biomedical Innovation, Health and Nutrition, Osaka 567-0085, Japan; Discovery Technology Laboratories, Mitsubishi Tanabe Pharma Corporation, Fujisawa, Kanagawa 251-8555, Japan*

Hitoshi Kawashima − *Laboratory of Bioinformatics, Artificial Intelligence Center for Health and Biomedical Research, National Institutes of Biomedical Innovation, Health and Nutrition, Osaka 567-0085, Japan*

Hiroshi Komura − *URA Center, Osaka City University, Osaka 545-0051, Japan*

Yayoi Natsume-Kitatani − *Laboratory of Bioinformatics, Artificial Intelligence Center for Health and Biomedical Research, National Institutes of Biomedical Innovation, Health and Nutrition, Osaka 567-0085, Japan*

Kenji Mizuguchi − *Laboratory of Bioinformatics, Artificial Intelligence Center for Health and Biomedical Research, National Institutes of Biomedical Innovation, Health and Nutrition, Osaka 567-0085, Japan; Laboratory of In-Silico Drug Design, Center of Drug Design Research, National Institutes of Biomedical Innovation, Health and Nutrition, Osaka 567-0085, Japan;* orcid.org/0000-0003-3021-7078

Complete contact information is available at: https://pubs.acs.org/10.1021/acs.jmedchem.0c02011

Author Contributions

[#]R.W. and T.E. contributed equally.

Notes

The authors declare no competing financial interest.

■ ACKNOWLEDGMENTS

This work was conducted as part of the "Development of a Drug Discovery Informatics System" supported by the Japan Agency for Medical Research and Development (AMED). We thank Dr. Chioko Nagao at Osaka University for extending cooperation in facilitating data collection. We also thank Daisuke Sato in Lifematics Inc. for helping with the creation of the web interface. Finally, we would like to thank Dr. Lokesh Tripathi and Editage (www.editage.jp) for English language editing.

■ ABBREVIATIONS

ANN, artificial neural network; apK_a, the most acidic pK_a; BBB, blood−brain barrier; BCEC, brain capillary endothelial cells; BCRP, breast cancer resistance protein; bpK_a, the most basic pK_a; CSF, cerebrospinal fluid; CNS, central nervous system; $f_{u,brain}$, fraction unbound in brain homogenate; $f_{u,p}$, fraction unbound in plasma; GB, gradient boosting; KO, knock out; $K_{p,brain}$, brain-to-plasma concentration ratio; $K_{p,uu,brain}$, unbound brain-to-plasma concentration ratio; MDR1, multidrug resistance 1; MSE, mean square error; *n*AromAtoms, the number of aromatic atoms; *n*AromBonds, the number of aromatic bonds; NER, net efflux ratio; *n*Rots, the number of rotatable bonds; OATP, organic anion-transporting polypeptide; P-gp, P-glycoprotein; Rb, blood to plasma concentration ratio; RF, random forest; SDF, structure data file; SVM, support vector machine; WT, wild-type

■ REFERENCES

(1) Palmer, A. M.; Alavijeh, M. S. Translational CNS Medicines Research. *Drug Discovery Today* **2012**, *17*, 1068−1078.

(2) Lin, J. H.; Yamazaki, M. Role of P-glycoprotein in Pharmacokinetics: Clinical Implications. *Clin. Pharmacokinet.* **2003**, *42*, 59−98.

(3) Esaki, T.; Ohashi, R.; Watanabe, R.; Natsume-Kitatani, Y.; Kawashima, H.; Nagao, C.; Mizuguchi, K. Computational Model to Predict the Fraction of Unbound Drug in the Brain. *J. Chem. Inf. Model.* **2019**, *59*, 3251−3261.

(4) Watanabe, R.; Esaki, T.; Kawashima, H.; Natsume-Kitatani, Y.; Nagao, C.; Ohashi, R.; Mizuguchi, K. Predicting Fraction Unbound in Human Plasma from Chemical Structure: Improved Accuracy in the Low Value Ranges. *Mol. Pharm.* **2018**, *15*, 5302−5311.

(5) Ohashi, R.; Watanabe, R.; Esaki, T.; Taniguchi, T.; Torimoto-Katori, N.; Watanabe, T.; Ogasawara, Y.; Takahashi, T.; Tsukimoto, M.; Mizuguchi, K. Development of Simplified in Vitro P-glycoprotein Substrate Assay and in Silico Prediction Models to Evaluate Transport Potential of P-glycoprotein. *Mol. Pharm.* **2019**, *16*, 1851−1863.

(6) Rodgers, T.; Leahy, D.; Rowland, M. Physiologically Based Pharmacokinetic Modeling 1: Predicting the Tissue Distribution of Moderate-to-Strong Bases. *J. Pharm. Sci.* **2005**, *94*, 1259−1276.

(7) Rodgers, T.; Rowland, M. Physiologically Based Pharmacokinetic Modelling 2: Predicting the Tissue Distribution of Acids, Very Weak Bases, Neutrals and Zwitterions. *J. Pharm. Sci.* **2006**, *95*, 1238−1257.

(8) Summerfield, S. G.; Stevens, A. J.; Cutler, L.; del Carmen Osuna, M.; Hammond, B.; Tang, S.-P.; Hersey, A.; Spalding, D. J.; Jeffrey, P. Improving the in Vitro Prediction of in Vivo Central Nervous System Penetration: Integrating Permeability, P-glycoprotein Efflux, and Free Fractions in Blood and Brain. *J. Pharmacol. Exp. Ther.* **2006**, *316*, 1282−1290.

(9) Uchida, Y.; Ohtsuki, S.; Kamiie, J.; Terasaki, T. Blood-Brain Barrier (BBB) Pharmacoproteomics: Reconstruction of in Vivo Brain Distribution of 11 P-glycoprotein Substrates Based on the BBB Transporter Protein Concentration, in Vitro Intrinsic Transport Activity, and Unbound Fraction in Plasma and Brain in Mice. *J. Pharmacol. Exp. Ther.* **2011**, *339*, 579−588.

(10) Ohtsuki, S.; Uchida, Y.; Kubo, Y.; Terasaki, T. Quantitative Targeted Absolute Proteomics-Based Adme Research as a New Path to Drug Discovery and Development: Methodology, Advantages, Strategy, and Prospects. *J. Pharm. Sci.* **2011**, *100*, 3547−3559.

(11) Kamiie, J.; Ohtsuki, S.; Iwase, R.; Ohmine, K.; Katsukura, Y.; Yanai, K.; Sekine, Y.; Uchida, Y.; Ito, S.; Terasaki, T. Quantitative Atlas of Membrane Transporter Proteins: Development and Application of a Highly Sensitive Simultaneous LC/MS/MS Method Combined with Novel in-Silico Peptide Selection Criteria. *Pharm. Res.* **2008**, *25*, 1469−1483.

(12) Uchida, Y.; Ohtsuki, S.; Katsukura, Y.; Ikeda, C.; Suzuki, T.; Kamiie, J.; Terasaki, T. Quantitative Targeted Absolute Proteomics of Human Blood-Brain Barrier Transporters and Receptors. *J. Neurochem.* **2011**, *117*, 333−345.

(13) Ito, K.; Uchida, Y.; Ohtsuki, S.; Aizawa, S.; Kawakami, H.; Katsukura, Y.; Kamiie, J.; Terasaki, T. Quantitative Membrane Protein Expression at the Blood-Brain Barrier of Adult and Younger Cynomolgus Monkeys. *J. Pharm. Sci.* **2011**, *100*, 3939−3950.

(14) Agarwal, S.; Uchida, Y.; Mittapalli, R. K.; Sane, R.; Terasaki, T.; Elmquist, W. F. Quantitative Proteomics of Transporter Expression in Brain Capillary Endothelial Cells Isolated from P-glycoprotein (P-gp), Breast Cancer Resistance Protein (BCRP), and P-gp/BCRP Knockout Mice. *Drug Metab. Dispos.* **2012**, *40*, 1164−1169.

(15) Hoshi, Y.; Uchida, Y.; Tachikawa, M.; Inoue, T.; Ohtsuki, S.; Terasaki, T. Quantitative Atlas of Blood-Brain Barrier Transporters, Receptors, and Tight Junction Proteins in Rats and Common Marmoset. *J. Pharm. Sci.* **2013**, *102*, 3343−3355.

(16) Esaki, T.; Watanabe, R.; Kawashima, H.; Ohashi, R.; Natsume-Kitatani, Y.; Nagao, C.; Mizuguchi, K. Data Curation Can Improve the Prediction Accuracy of Metabolic Intrinsic Clearance. *Mol. Inf.* **2019**, *38*, 1800086.

(17) Uchida, Y.; Yagi, Y.; Takao, M.; Tano, M.; Umetsu, M.; Hirano, S.; Usui, T.; Tachikawa, M.; Terasaki, T. Comparison of Absolute Protein Abundances of Transporters and Receptors among Blood-Brain Barriers at Different Cerebral Regions and the Blood-Spinal Cord Barrier in Humans and Rats. *Mol. Pharm.* **2020**, *17*, 2006−2020.

(18) Kikuchi, R.; de Morais, S. M.; Kalvass, J. C. In Vitro P-Glycoprotein Efflux Ratio Can Predict the in Vivo Brain Penetration Regardless of Biopharmaceutics Drug Disposition Classification System Class. *Drug Metab. Dispos.* **2013**, *41*, 2012−2017.

(19) Takeuchi, T.; Yoshitomi, S.; Higuchi, T.; Ikemoto, K.; Niwa, S.-I.; Ebihara, T.; Katoh, M.; Yokoi, T.; Asahi, S. Establishment and Characterization of the Transformants Stably-Expressing MDR1 Derived from Various Animal Species in LLC-PK1. *Pharm. Res.* **2006**, *23*, 1460−1472.

(20) Wang, Y.-H.; Li, Y.; Yang, S.-L.; Yang, L. Classification of Substrates and Inhibitors of P-glycoprotein Using Unsupervised Machine Learning Approach. *J. Chem. Inf. Model.* **2005**, *45*, 750−757.

(21) Dolgikh, E.; Watson, I. A.; Desai, P. V.; Sawada, G. A.; Morton, S.; Jones, T. M.; Raub, T. J. Qsar Model of Unbound Brain-to-Plasma Partition Coefficient, Kp,Uu,Brain: Incorporating P-glycoprotein Efflux as a Variable. *J. Chem. Inf. Model.* **2016**, *56*, 2225−2233.

(22) Liu, H.; Dong, K.; Zhang, W.; Summerfield, S. G.; Terstappen, G. C. Prediction of Brain:Blood Unbound Concentration Ratios in CNS Drug Discovery Employing in Silico and in Vitro Model Systems. *Drug Discovery Today* **2018**, *23*, 1357−1372.

(23) Eechoute, K.; Sparreboom, A.; Burger, H.; Franke, R. M.; Schiavon, G.; Verweij, J.; Loos, W. J.; Wiemer, E. A. C.; Mathijssen, R. H. J. Drug Transporters and Imatinib Treatment: Implications for Clinical Practice. *Clin. Cancer Res.* **2011**, *17*, 406−415.

(24) Chen, Y.; Agarwal, S.; Shaik, N. M.; Chen, C.; Yang, Z.; Elmquist, W. F. P-glycoprotein and Breast Cancer Resistance Protein Influence Brain Distribution of Dasatinib. *J. Pharmacol. Exp. Ther.* **2009**, *330*, 956−963.

(25) Liu, H.; Yu, N.; Lu, S.; Ito, S.; Zhang, X.; Prasad, B.; He, E.; Lu, X.; Li, Y.; Wang, F.; Xu, H.; An, G.; Unadkat, J. D.; Kusuhara, H.; Sugiyama, Y.; Sahi, J. Solute Carrier Family of the Organic Anion-Transporting Polypeptides 1A2- Madin-Darby Canine Kidney II: A Promising in Vitro System to Understand the Role of Organic Anion-Transporting Polypeptide 1A2 in Blood-Brain Barrier Drug Penetration. *Drug Metab. Dispos.* **2015**, *43*, 1008−1018.

(26) Zhang, D.; He, K.; Herbst, J. J.; Kolb, J.; Shou, W.; Wang, L.; Balimane, P. V.; Han, Y.-H.; Gan, J.; Frost, C. E.; Humphreys, W. G. Characterization of Efflux Transporters Involved in Distribution and Disposition of Apixaban. *Drug Metab. Dispos.* **2013**, *41*, 827−835.

(27) Chen, X.; Slattengren, T.; de Lange, E. C. M.; Smith, D. E.; Hammarlund-Udenaes, M. Revisiting Atenolol as a Low Passive Permeability Marker. *Fluids Barriers CNS* **2017**, *14*, 30.

(28) Iisalo, E. Clinical Pharmacokinetics of Digoxin. *Clin. Pharmacokinet.* **1977**, *2*, 1−16.

https://dx.doi.org/10.1021/acs.jmedchem.0c02011
J. Med. Chem. 2021, 64, 2725−2738

(29) Noël, F.; Azalim, P.; do Monte, F. M.; Quintas, L. E. M.; Katz, A.; Karlish, S. J. D. Revisiting the Binding Kinetics and Inhibitory Potency of Cardiac Glycosides on Na(+),K(+)-ATPase (a1b1): Methodological Considerations. *J. Pharmacol. Toxicol. Methods* **2018**, *94*, 64−72.

(30) Friden, M.; Winiwarter, S.; Jerndal, G.; Bengtsson, O.; Wan, H.; Bredberg, U.; Hammarlund-Udenaes, M.; Antonsson, M. Structure-Brain Exposure Relationships in Rat and Human Using a Novel Data Set of Unbound Drug Concentrations in Brain Interstitial and Cerebrospinal Fluids. *J. Med. Chem.* **2009**, *52*, 6233−6243.

(31) Spreafico, M.; Jacobson, M. P. In Silico Prediction of Brain Exposure: Drug Free Fraction, Unbound Brain to Plasma Concentration Ratio and Equilibrium Half-Life. *Curr. Top. Med. Chem.* **2013**, *13*, 813−820.

(32) Loryan, I.; Sinha, V.; Mackie, C.; Van Peer, A.; Drinkenburg, W. H.; Vermeulen, A.; Heald, D.; Hammarlund-Udenaes, M.; Wassvik, C. M. Molecular Properties Determining Unbound Intracellular and Extracellular Brain Exposure of CNS Drug Candidates. *Mol. Pharm.* **2015**, *12*, 520−532.

(33) Kodaira, H.; Kusuhara, H.; Fujita, T.; Ushiki, J.; Fuse, E.; Sugiyama, Y. Quantitative Evaluation of the Impact of Active Efflux by P-glycoprotein and Breast Cancer Resistance Protein at the Blood-Brain Barrier on the Predictability of the Unbound Concentrations of Drugs in the Brain Using Cerebrospinal Fluid Concentration as a Surrogate. *J. Pharmacol. Exp. Ther.* **2011**, *339*, 935−944.

(34) Liu, X.; Smith, B. J.; Chen, C.; Callegari, E.; Becker, S. L.; Chen, X.; Cianfrogna, J.; Doran, A. C.; Doran, S. D.; Gibbs, J. P.; Hosea, N.; Liu, J.; Nelson, F. R.; Szewc, M. A.; Van Deusen, J. Evaluation of Cerebrospinal Fluid Concentration and Plasma Free Concentration as a Surrogate Measurement for Brain Free Concentration. *Drug Metab. Dispos.* **2006**, *34*, 1443−1447.

(35) Ueda, K.; Okamura, N.; Hirai, M.; Tanigawara, Y.; Saeki, T.; Kioka, N.; Komano, T.; Hori, R. Human P-Glycoprotein Transports Cortisol, Aldosterone, and Dexamethasone, but Not Progesterone. *J. Biol. Chem.* **1992**, *267*, 24248−24252.

(36) Tanigawara, Y.; Okamura, N.; Hirai, M.; Yasuhara, M.; Ueda, K.; Kioka, N.; Komano, T.; Hori, R. Transport of Digoxin by Human P-glycoprotein Expressed in a Porcine Kidney Epithelial Cell Line (LLC-PK1). *J. Pharmacol. Exp. Ther.* **1992**, *263*, 840−845.

(37) Uchida, Y.; Tachikawa, M.; Obuchi, W.; Hoshi, Y.; Tomioka, Y.; Ohtsuki, S.; Terasaki, T. A Study Protocol for Quantitative Targeted Absolute Proteomics (QTAP) by LC-MS/MS: Application for Inter-Strain Differences in Protein Expression Levels of Transporters, Receptors, Claudin-5, and Marker Proteins at the Blood−Brain Barrier in ddY, FVB, and C57BL/6J Mice. *Fluids Barriers CNS* **2013**, *10*, 21.

https://dx.doi.org/10.1021/acs.jmedchem.0c02011
J. Med. Chem. 2021, 64, 2725−2738